Expanded View Figures

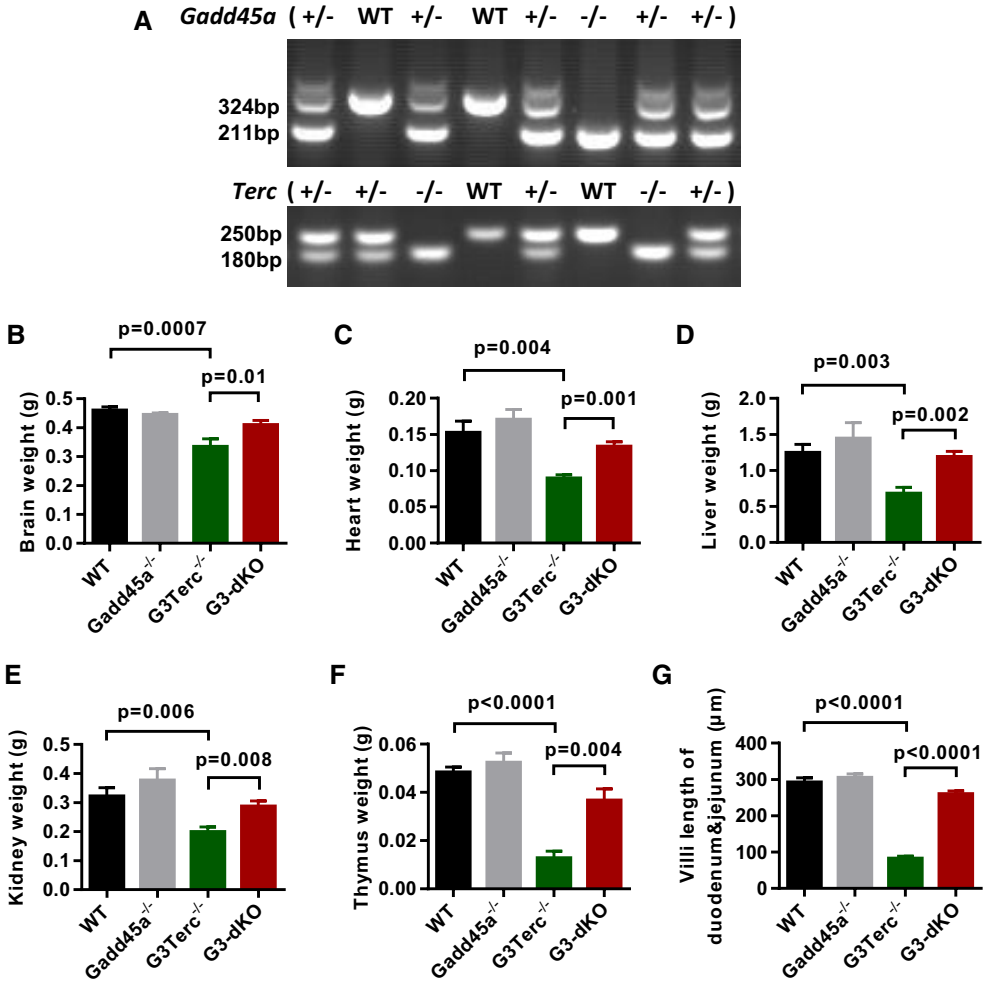

Figure EV1. *Gadd45a* deletion prevents overall organ atrophy of aged G3*Terc*$^{-/-}$ mice.

A Representative example of mice genotyping. Upper panel is genotyping of *Gadd45a* and lower panel is genotyping of *Terc* gene.

B–F The average weights of brain (B), heart (C), liver (D), kidney (E), and thymus (F) from 6- to 7-month-old mice (n = 5–12 mice/group).

G Quantification of villi length in duodenum and jejunum of small intestines (n = 5–6 mice per genotype).

Data information: Data are presented as mean ± SEM. *P*-values were calculated with unpaired two-tailed Student's *t*-test.

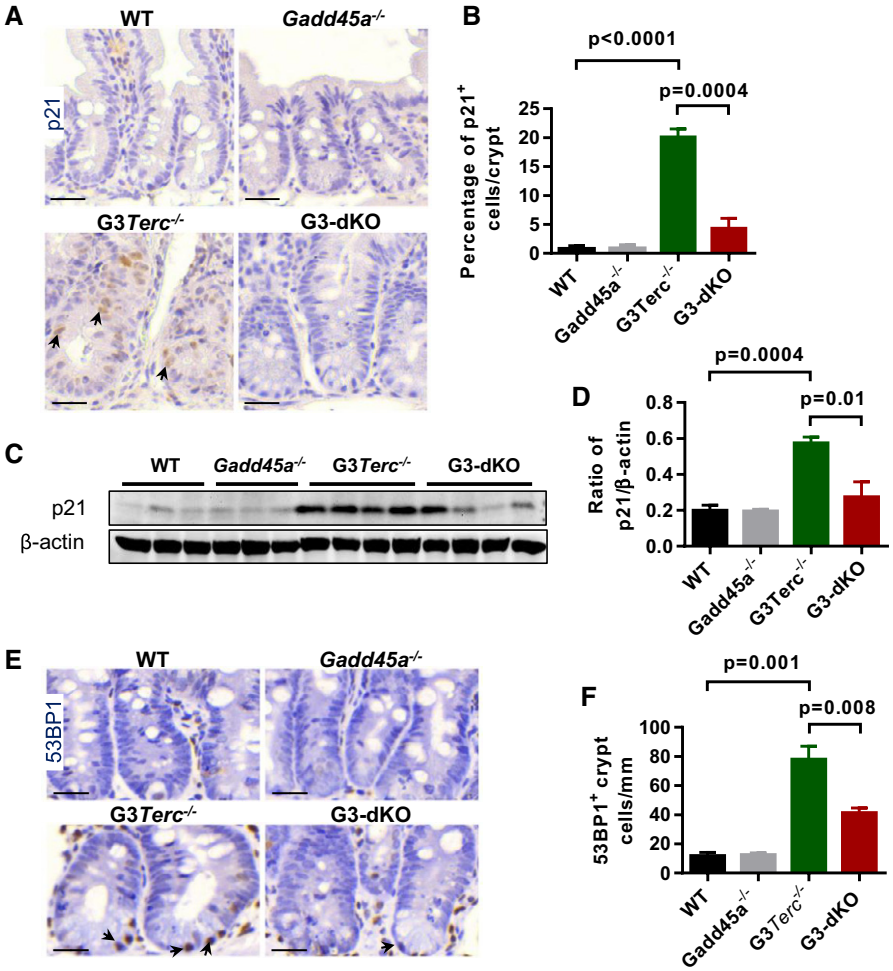

Figure EV2. *Gadd45a* deletion attenuated DDR signaling in the intestine basal crypts of G3-dKO mice.

A Representative images of small intestine sections stained with p21 antibody. Arrows indicate the positive nuclear staining of p21 antibody.

B Quantification of the percentage of p21-positive crypt cells (n = 4–6 of 7-month-old mice per genotype).

C Western blotting analysis of p21 protein expression in mouse intestine crypt lysates from WT, *Gadd45a*$^{-/-}$, G3*Terc*$^{-/-}$, and G3-dKO mice.

D Quantification of p21 protein expression; β-actin protein level was used as the loading control (n = 3–4 mice per genotype).

E Representative images of small intestine crypt sections stained with antibody against 53BP1. Arrows mark the positive nuclear staining of 53BP1 antibody.

F Quantification of frequencies of 53BP1-positive crypt cells (n = 4–6 of 7-month-old mice per genotype).

Data information: All scale bars represent 25 μm. Data are presented as mean ± SEM. P-values were calculated with unpaired two-tailed Student's t-test.

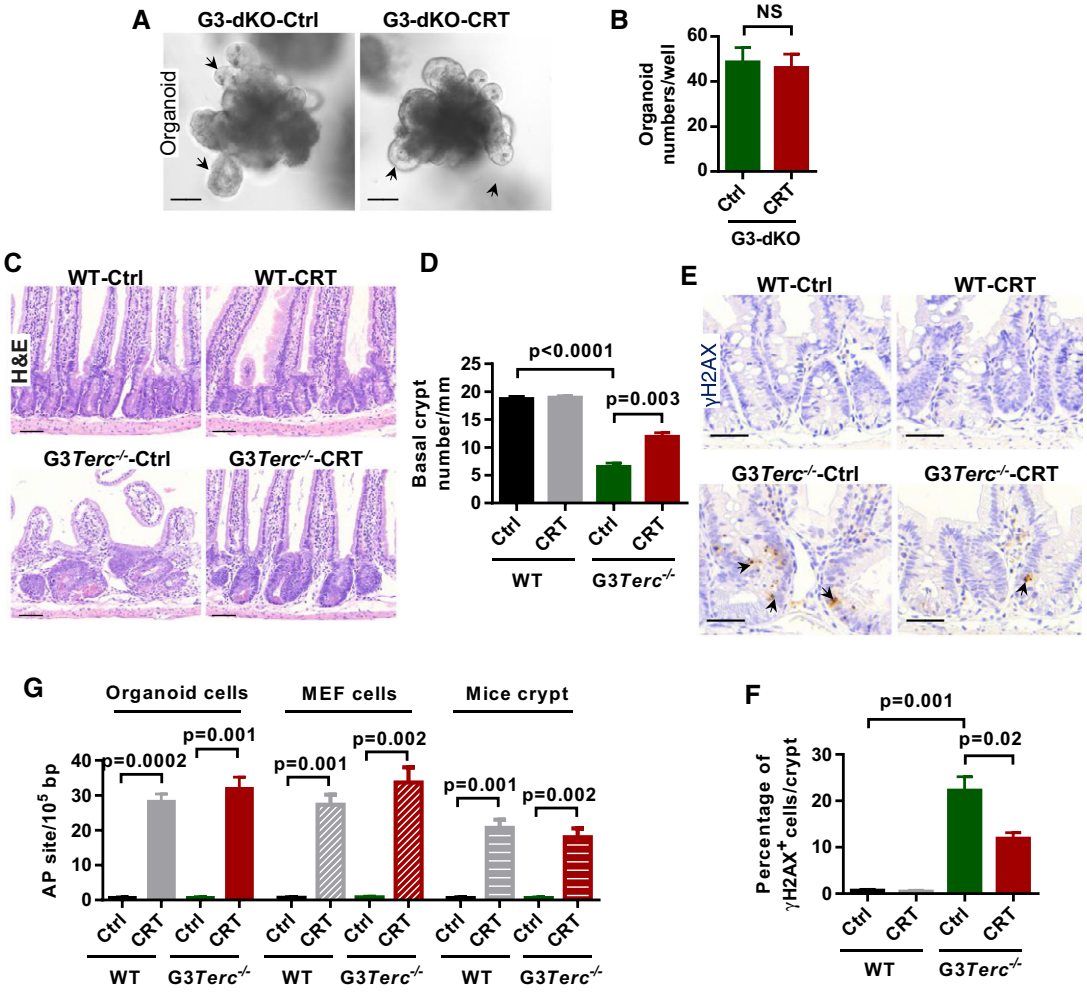

Figure EV3. APE1 inhibition rescues intestine maintenance in G3*Terc*$^{-/-}$ mice.

A Representative images of small intestine organoids from G3-dKO mice incubated with or without APE1 inhibitor CRT0044876 (CRT, 10 μM) treatment. Arrows indicate the crypt-like structure in organoid cultures.

B Quantification of organoid number (per well) from crypt cultures (n = 3–4 mice per treatment).

C H&E-stained small intestine sections from 7-month-old mice treated with or without APE1 inhibitor CRT0044876 (CRT).

D Quantification of the number of small intestine basal crypts (n = 4 mice per group).

E Representative images of γH2AX antibody staining on small intestine sections from WT and G3*Terc*$^{-/-}$ mice treated with or without APE1 inhibitor CRT0044876 (CRT). Arrows indicate γH2AX-positive nuclei.

F Quantification of the percentage of γH2AX-positive cells per small intestine crypt (n = 4 mice per group).

G Inhibition efficiency of enzyme activity by using APE1 inhibitor CRT0044876 (CRT). Relative AP site accumulation was used as an indicator for enzyme activity inhibition. Organoid and MEF cells were treated with and without CRT0044876. Crypt isolated from WT and G3*Terc*$^{-/-}$ mice treated with and without CRT0044876 (n = 3 replicates per group).

Data information: Scale bars represent 50 μm in (A and C); 25 μm in (E). Data are presented as mean ± SEM. P-values were calculated with unpaired two-tailed Student's t-test.

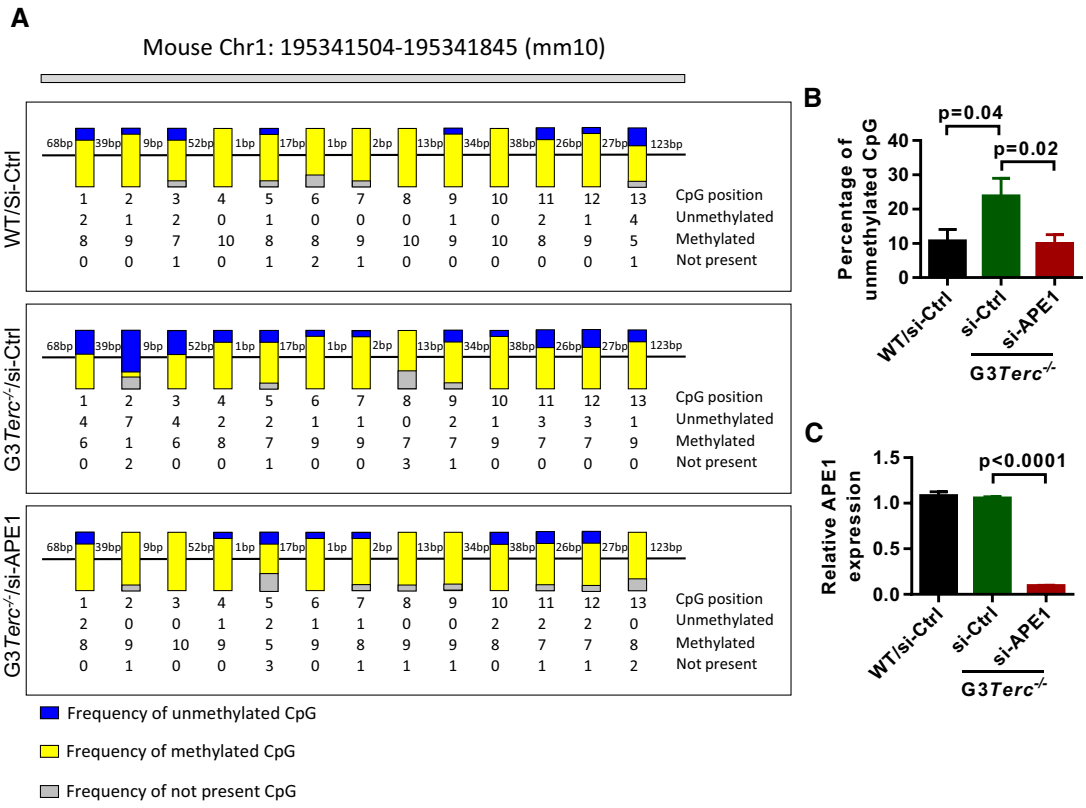

Figure EV4. APE1 knockdown reduces DNA demethylation in the sub-telomeric region of G3*Terc*$^{-/-}$ mice.

A The methylation status of CpG island in sub-telomeric regions of chromosome 1q. gDNAs were isolated from MEF cells treated with and without APE1 siRNA and analyzed by bisulfite sequencing. Yellow and blue bars indicate the frequencies of methylated and unmethylated CpG islands, respectively.

B Quantification of the percentage of unmethylated CpG islands in (A) (Data was quantified from 13 CpG islands and each for 10 colony replicates).

C Quantification of APE1 knockdown efficiency in G3*Terc*$^{-/-}$ cells (n = 3 replicates per group).

Data information: Data are presented as mean ± SEM. P-values were calculated with unpaired two-tailed Student's t-test.

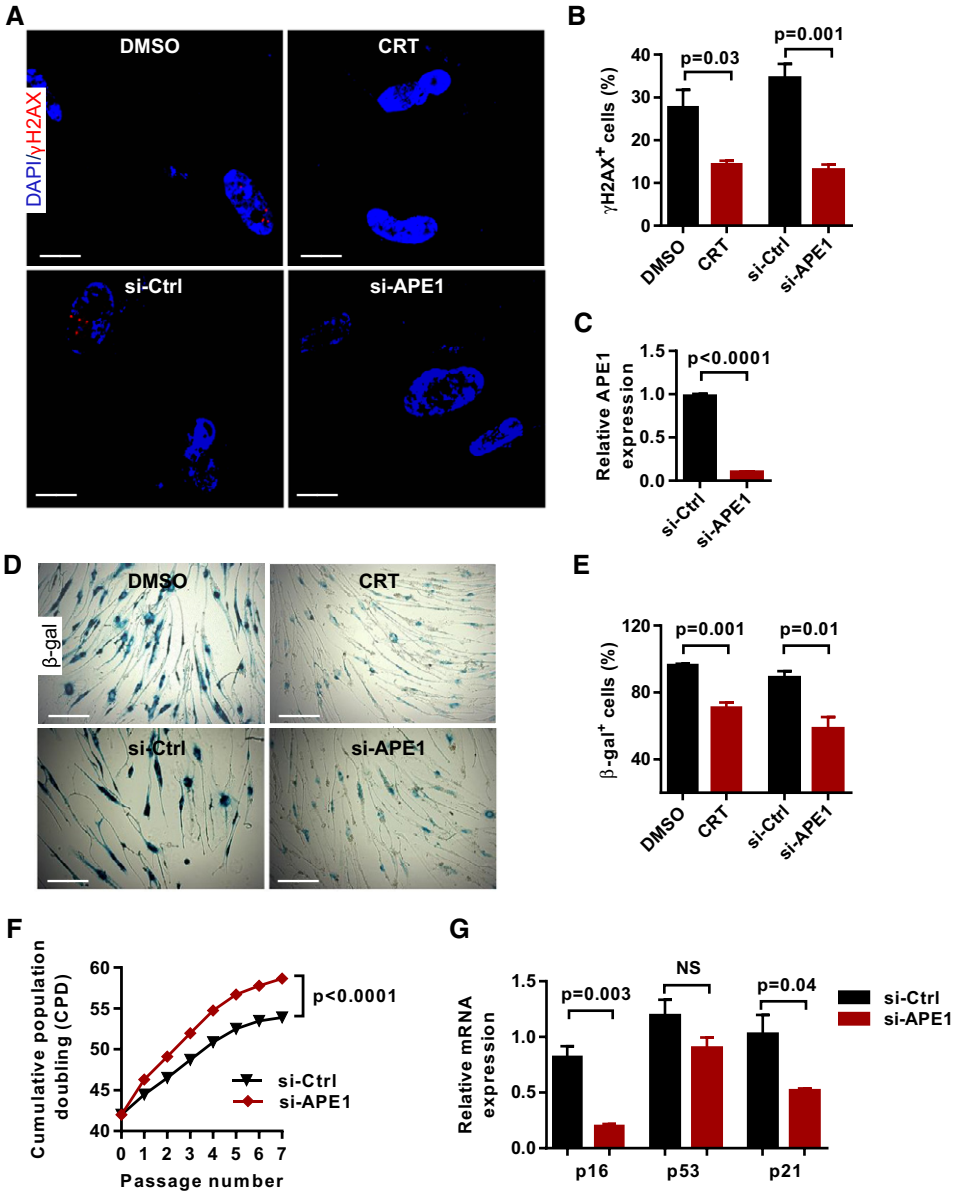

Figure EV5. APE1 inhibition and knockdown reduce DNA damage response and replicative senescence in human cells.

A Representative images of γH2AX antibody staining on human fibroblasts WI38 treated with APE1 inhibitor CRT0044876 (CRT, 100 μM) and APE1 siRNA (si-APE1) at passage 48 (DNA is stained with DAPI).

B Quantification of γH2AX-positive cells in (A) (triplicates per group).

C The knockdown efficiency of APE1 in human fibroblast WI38 cells (n = 3 replicates per group).

D Representative images of β-gal staining in human fibroblasts treated with APE1 inhibitor CRT0044876 (CRT, 100 μM) and APE1 siRNA at passage 48.

E Quantification of β-gal-positive cells in human fibroblasts treated with APE1 inhibitor CRT0044876 (CRT) and APE1 siRNA treatments (triplicates per group).

F The growth curves of human WI38 fibroblasts treated with control and APE1 siRNA (n = 3 replicates per group).

G The relative mRNA expression of senescence-related genes (p16, p53, and p21) in WI38 fibroblasts after APE1 siRNA treatment (n = 3 replicates per group).

Data information: Scale bars represent 25 μm in (A) and 150 μm in (D). Data are presented as mean ± SEM. P-values were calculated with unpaired two-tailed Student's t-test.